

Natural Convection in a Vertical Rectangular Enclosure

Manar Salih Mahdi

University of Tikrit/ College of Engineering/ Dep. of Mechanical Engineering

manar_salih@yahoo.com

Received date: 6/5/2012

Accepted date:1/12/2013

Abstract

In this paper an experimental work has been conducted to investigate the influence of heating the lower half and cooling the upper half of vertical surface of a rectangular enclosure on natural convection. The enclosure length is (100 cm) with a square cross section (10×10 cm). The tests are done for three mass flow rates (0, 0.003 and 0.03 kg/sec) and five heat fluxes (48, 187, 400, 706 and 1080 W/m²). The hottest region formed is observed at ($\frac{x}{L} = 0.67$) where the lowest Nu_x is found while the coldest region is observed at ($\frac{x}{L} = 0.33$) where the highest Nu_x is found. Increasing the water mass flow rate enhances the heat transfer. The same thing happens with increasing the heat flux. A correlation is found to relate Nu with Ra ($Nu = 0.216 Ra^{1/4}$) for ($4 \times 10^5 \leq Ra \leq 4 \times 10^6$). Both the experimental results and the correlation found are compared with a previous work and fair agreement is found.

Keywords: natural convection, vertical enclosure, heating and cooling.

الحمل الحر في حيز شاقولي مستطيل

منار صالح مهدي

جامعة تكريت - كلية الهندسة - قسم الهندسة الميكانيكية

تاريخ قبول البحث: 2013/12/1

تاريخ استلام البحث: 2012/5/6

الخلاصة

تم في هذا البحث إجراء دراسة عملية لأختبار تأثير تسخين النصف السفلي لسطح شاقولي وتبريد النصف العلوي في حيز مستطيل على الحمل الطبيعي. طول الحيز (100 cm) وهو ذو مقطع مربع (10×10 cm). أجريت الاختبارات لثلاث معدلات تدفق كتلية (0 و 0.003 و 0.03 kg/sec) وخمس قيم للفيض الحراري (48 و 187 و 400 و 706 و 1080 W/m²). لوحظ تشكل أدفء منطقة عند ($\frac{x}{L} = 0.67$) حيث توجد أقل قيمة لـ Nu_x بينما لوحظت أبرد منطقة عند ($\frac{x}{L} = 0.33$) حيث توجد أعلى قيمة لـ Nu_x . زيادة التدفق الكتلي للماء يحسن انتقال الحرارة، الشيء نفسه يحدث عند زيادة الفيض الحراري. أوجدت معادلة ترابطية لربط Nu مع Ra ($Nu = 0.23 (0.778 Ra)^{1/4}$) للمدى ($4 \times 10^5 \leq Ra \leq 4 \times 10^6$). قورنت كل من النتائج العملية والعلاقة الترابطية مع عمل سابق ووجد تقارب جيد بينها.

الكلمات الدالة: حمل حر، حيز شاقولي، تسخين وتبريد.

Introduction

Natural convection occurs due to the influence of buoyant forces on fluids when there is a temperature or concentration induced density gradient within the fluid. Natural convection in enclosures studies had wide scope such as the geometry characteristic of enclosures, the fluid occupying the enclosure, the nature of the fluid flow, orientation of the enclosure [1]. Natural convection in a vertical enclosure has received considerable attention by many researchers because of its wide applications in industrial works, solar collectors and electronic

cooling. Desrayaud and Frichera [2] had investigated numerically laminar natural convective flows in a vertical isothermal channel with two rectangular ribs, symmetrically located on each wall. The control volume method was used to solve the governing elliptic equations and the SIMPLER algorithm for the velocity- pressure coupling was employed. Their results showed how on moving the ribs towards the outlet, the mean Nusselt number increases as the distance of the ribs from the inlet increases, but only for high values of the channel Rayleigh number. They found that the best position of the ribs for heat extraction depends on the magnitude of Rayleigh number. The inlet flow rate always decreases when the distance of the obstruction from the leading edge of the channel increases at any Rayleigh number. They indicated that at any location of the ribs the mean Nusselt number behavior at high Rayleigh number was the same for isothermal and adiabatic ribs, where the mean Nusselt number for the adiabatic obstructions was lower. Also they found that the ribs length had a limited influence on the heat transfer while increasing its width decreases the mass flow rate and the heat transfer especially if more than half of the opening is obstructed.

The constructal method was used by da Silva et. al [3] to determine the optimal distribution and sizes of discrete heat sources in a vertical open channel cooled by natural convection. They considered two classes of geometries: (i) heat sources with fixed size and fixed heat flux, and (ii) single heat source with variable size and fixed total heat current. The numerical results showed that the spacings between discrete heat sources of fixed size and heat flux attached to an open channel with natural convection can be optimized for maximal global thermal conductance. Finite- length spacings are found only in configurations with two or more heat sources, and they occurred only between the heat sources positioned closest to the exit plane of the open channel. Also the numerical results showed that the global thermal conductance increases with Rayleigh number, the size of the heat source and number of heat sources, beside it increases as the number of optimally positioned heat source placed in the open channel increases. They predicted from their paper that optimized complexity is a promising feature, even though diminishing returns set in as complexity increases.

Tanda [4] had investigated experimentally the effect of repeated horizontal protrusions on the free convection heat transfer in a vertical, asymmetrically heated channel. The protrusions had a square section and are made of a low- thermal conductivity material. The experiments were conducted by varying the number of the protrusions over the heated surface and the aspect ratio of the channel. The distribution of the local heat transfer coefficient, measured by the schlieren optical technique was clearly affected by the presence of ribs on the heated wall.

When the channel spacing was relatively large the incoming fresh air from the core upmoving current leads to a relative maximum in heat transfer coefficient value generally higher than that of the smooth surface at the same elevation. It was found that if the inter-rib distance was too small, the local heat transfer enhancement occurred on a little portion of the ribbed surface. As the channel spacing was reduced (up to only 5% of the height), the heat transfer performance of the ribbed surface (as compared to the unribbed surface) is strongly reduced (from 18% to 43%). When repeated ribs were located on the heated plate, the inter-rib distance has to be properly selected in order to prevent the local heat transfer enhancement in the inter-rib region from being offset by the decrease in the stagnation zones immediately upstream and downstream of each rib.

A numerical and experimental study was carried by Bairiet. al [5] to determine the thermal behavior in a cavity where the electronic assembly was a wall made of discrete hot sources under dynamic operation. The treated cavity is an air-filled cube that consists of two active opposing walls connected by a channel. The channel was adiabatic and the two active walls were responsible of the natural convection flow inside the cavity. The cold wall was maintained isothermal at temperature T_c . The second active wall consisted of 5 bands of which 3 were heated and maintained at T_h . separated by 2 other adiabatic bands. The active walls can be vertical and tilted an angle with respect to the gravity direction. Finite volumes method was used to carry out calculations in steady- state regime. The dynamic and thermal aspects were examined for several configurations obtained while varying the difference of temperatures (T_h-T_c) and the inclination angle of the cavity. Their study covered a wide range of Rayleigh number from 10^3 to 3×10^8 and inclination angles between 0° and 360° . They compared their numerical results with the experimental measurements and deviations encountered were slight. The temperature distribution on the passive walls originated by the natural convection flow had the same aspect in both cases and the computed values differ from the calculated ones only in about 0.4°C on average. They concluded that the heat exchanges occurred with different intensity on the three heated bands, but this difference tended to disappear when the angle of inclination increased and for high Rayleigh numbervalues. They found out that heat exchanges were 10% lower on average than those corresponding to cavities with an entirely isothermal hot plate.

Nimkar and Prayagi [6] had studied experimentally natural convection in horizontal plate with vertical channels. The varied parameters during the experimentation were heat input, aspect ratio (the ratio of gap of horizontal plate with respect to vertical plate and gap of horizontal

plate from bottom to top), and horizontal plate with and without V- slot. They found that with V-slots the rate of heat transfer enhanced considerably.

The present work investigates experimentally laminar natural convection in a vertical rectangular enclosure. All its surfaces were insulated except its left vertical side, where the lower half was heated and the upper half was cooled.

Experimental Work

The experimental rig shown in figure (1) – A- a photograph, B- a schematic drawing- is used to investigate the effect of heating the lower half and cooling the upper half of the left surface of a vertical enclosure on natural convection inside the enclosure. A rectangular enclosure with a square cross section area is made of galvanized iron oriented vertically is used. The enclosure thickness (δ) and width (B) are (10 cm), its length is (100 cm).

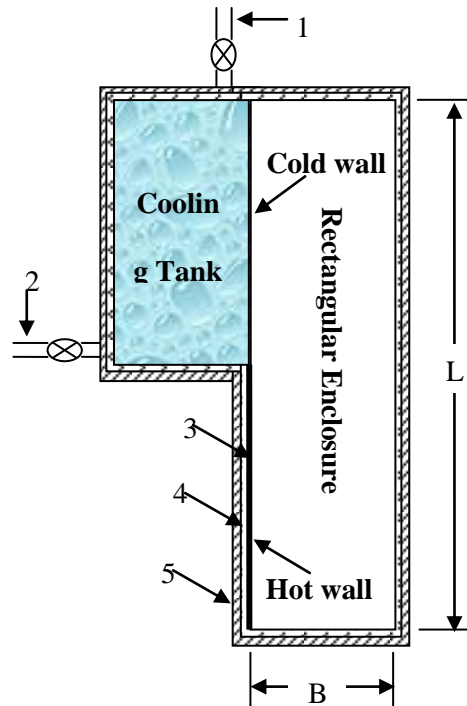
The lower half of the left surface test section was heated electrically using an electrical resistance of (5m) in length with a resistance ($1\Omega/m$). The heater is supplied with an alternative electrical power monitored via a variable voltage transformer. An ammeter is used to measure the current passes through the heater and a voltmeter to measure the voltage.

While the upper half is cooled by water using a cooling tank (10×10×50cm). The cooling water flow rate can be controlled by two valves one for inlet and another for outlet water from the cooling tank. The water mass flow rate is measured by using a (1000 ml) glass container and stop watch.



(A)

1- test section , 2- meter panel. 3- cooling tank. 4- valve. 5- voltage regular, 6- ammeter, 7- voltmeter.



(B)

1- inlet water valve, 2- outlet water valve, 3- thermal resistance, 4- thermal insulator, 5- fiber glass.

Figure (1)A photo graph (A) and a schematic drawing of the test section (B).

To reduce the heat losses the test section is thermally insulated with fiber glass of (1 cm) in thickness. The two ends of the apparatus section and other surfaces were insulated electrically and thermally using fiber glass.

Eighteen calibrated thermocouples (T- type) were used to measure the temperature: on the left heated and cooled surface (5 locations along the surface), the opposite vertical surface (5 locations along the surface), the temperature of the air along the center of the enclosure (5 locations), two thermocouples to measure the temperature of the inlet and outlet water from the cooling tank and a thermocouple to measure the laboratory ambient temperature.

Calculation Procedures

The test procedure can be listed as follow:-

- 1- Control the water mass flow rate by the inlet valve.
- 2- The test section is set to the proper voltage and this is achieved using a variable transformer.
- 3- After (1.5-2 hr) the system reaches the steady state condition. The enclosure surfaces temperatures, the inlet and outlet water temperatures, the water mass flow rate through the cooling tank, the laboratory temperature and the heater voltage and current have been registered.

The heat generated (Q_g) is dissipating from the enclosure surface by convection and radiation.

$$Q_g = \frac{I * V}{A_s} \quad \dots(1)$$

Where $A_s = 0.5B * L$

$$Q_g = q_c + q_r \quad \dots(2)$$

Where q_c and q_r , are the fraction of the heat flux dissipating from the enclosure surface by convection and radiation, respectively which can be calculated as Mohamed[10]:

$$q_r = \frac{\sigma(T_H^4 - T_C^4)}{\frac{2}{\varepsilon} - 1} \quad \dots(3)$$

Where ε is the surface emissivity of the enclosure and it is estimated as 0.3 for galvanized iron Siegel[8].

Where the quantity of the heat absorbed by water (Q_w) is calculated as follow Holman[9]:

$$Q_w = \dot{m}_w C_{pw} (T_{wo} - T_{wi}) \quad \dots(4)$$

Local convection heat transfer coefficient and local Nusselt number have been calculated indirectly measured respectively using the following equations Mohamed[10]:

$$h_x = \frac{q_c}{(T_{Hx} - T_{Cx})} \quad \dots(5)$$

$$Nu_x = \frac{h_x \cdot \delta}{k} \quad \dots(6)$$

Then the overall longitudinal average \bar{h} can calculated as flow Mohamed[10]:

$$\bar{h} = \sum_{x=1}^5 h_x / 5 \tag{7}$$

The non-dimensional overall average Nusselt and Rayleigh numbers are calculated as follow Mohamed[10]:

$$Nu = \frac{\bar{h} \delta}{k} \tag{8}$$

$$Ra = \frac{g \beta (T_{Hx} - T_{Cx}) \delta^3}{\nu \alpha} \tag{9}$$

Where all the air properties were indicated at the film temperature ($T_f = (T_H - T_C) / 2$).

Results and Discussion

Fifteen tests had been carried out for three mass flow rates of water (0, 0.003 and 0.03 kg/s) and five heat fluxes (48, 187, 400, 706 and 1080 W/m²). The previous tests have been repeated ones for each change in water mass flow rate.

To predict the present work results a comparison is made by the present experimental data at ($\dot{m} = 0$ kg/sec) with the proposed equation in Bejan and Kraus[7] as shown in figure (2).

Where the proposed equation is:

$$Nu = 0.22 \left(\frac{Pr}{0.2 + Pr} Ra \right)^{0.28} \left(\frac{H}{d} \right)^{-1/4} \tag{10}$$

For ($Ra > 10^3$, $2 < \frac{H}{d} < 10$, $Pr < 10^5$).

The maximum difference between the present work and the case above is (27 %) which can be accepted since this proposed equation is for a whole heated vertical surface but in the present work the vertical surface is partially heated.

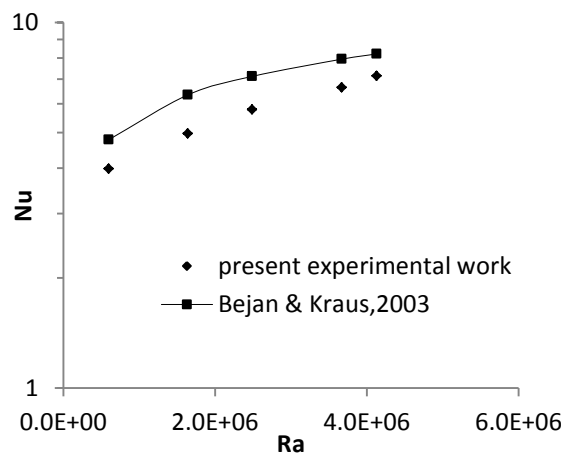


Figure (2) comparison between present experimental work with (Bejan & Kraus,2003) at ($\dot{m} = 0.0$ kg/s).

The effect of mass flow rate upon the temperature ratio at constant heat flux is shown in figures (3-7). The cold air in the cooled half gets heavier and tends to move downward so the temperature ratio decreases from ($\frac{x}{L} = 0.17$) to ($\frac{x}{L} = 0.33$) -the coldest region in the enclosure-, but after this point the temperature ratio rises – because of heating- to get its highest value at ($\frac{x}{L} = 0.67$) where the hottest area is formed. At ($\frac{x}{L} = 0.83$) the heating is almost started that's why temperature ratio decreases at ($\frac{x}{L} = 0.83$).

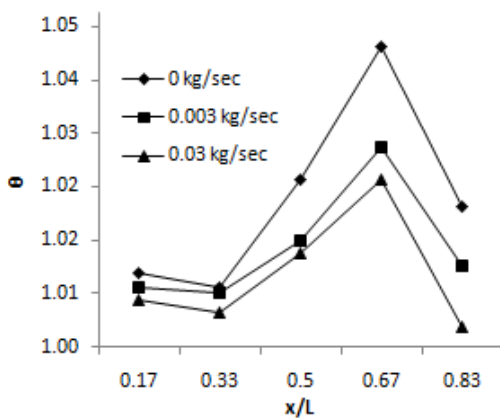


Figure (3) Effect of mass flow rate on the temp.ratio distribution along the enclosure at ($Q_g=48 \text{ W/m}^2$).

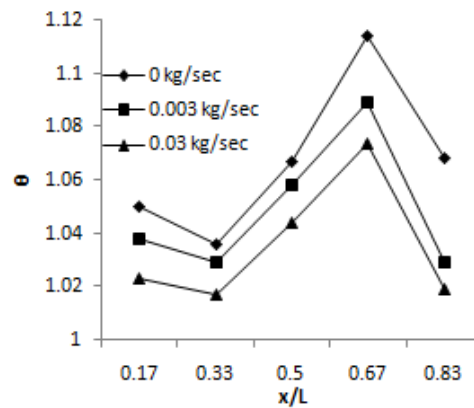


Figure (4) Effect of mass flow rate on the temp.ratio distribution along the enclosure at ($Q_g=187 \text{ W/m}^2$).

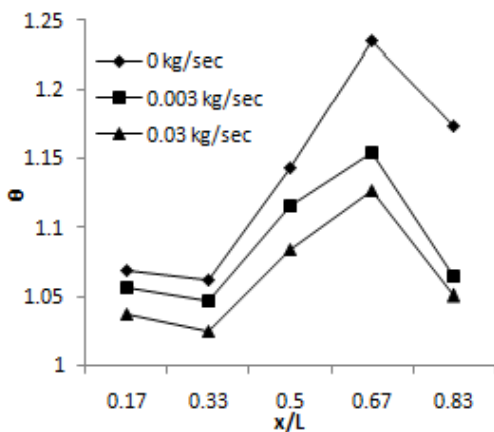


Figure (5) Effect of mass flow rate on the temp.ratio distribution along the enclosure at ($Q_g=400 \text{ W/m}^2$).

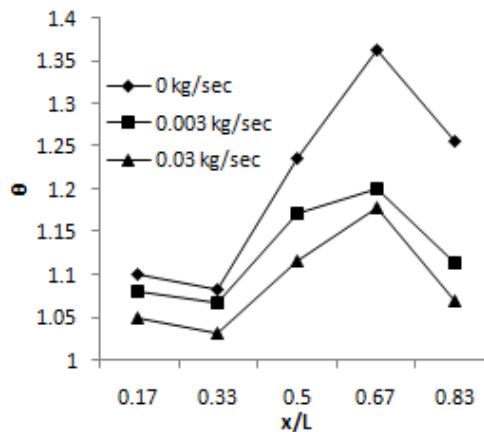


Figure (6) Effect of mass flow rate on the temp.ratio distribution along the enclosure at ($Q_g=706 \text{ W/m}^2$).

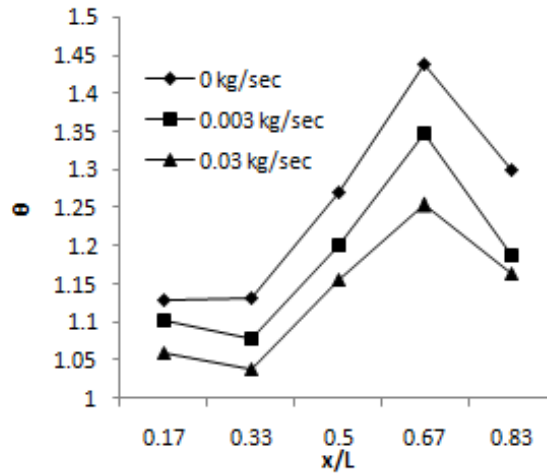


Figure (7) Effect of mass flow rate on the temp. ratio distribution along the enclosure at ($Q_g=1080 \text{ W/m}^2$).

Also it can be noticed that as the water flow rate increases the temperature ratio decreases, since more heat is absorbed by the water if its flow rate increases.

Figures (8-10) show the effect of changing heat flux on the temperature ratio. Adding more heat to the enclosure increases the temperature ratio. The temperature ratio distribution is still behaving the same behavior when changing the water mass flow rate along the enclosure.

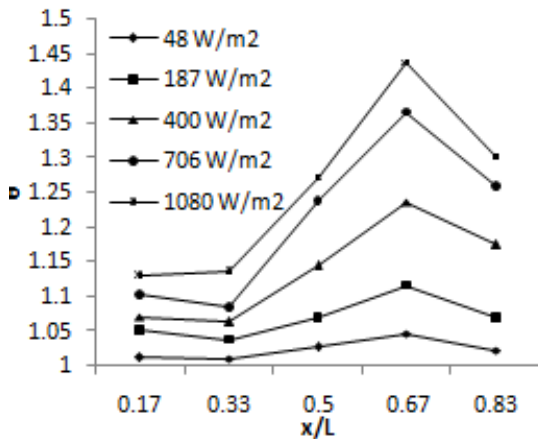


Figure (8) Effect of heat flux on the temp. ratio distribution along the enclosure at ($\dot{m} = 0 \text{ kg/s}$).

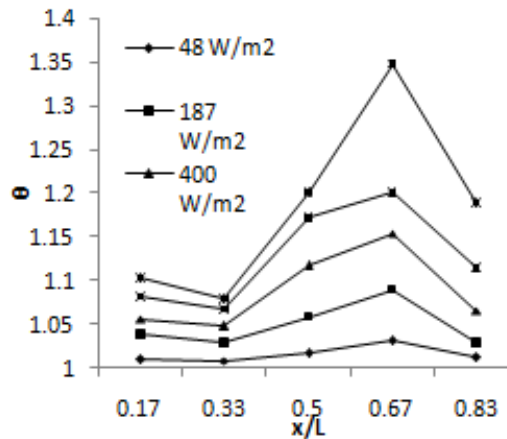


Figure (9) Effect of heat flux on the temp. ratio distribution along the enclosure at ($\dot{m} = 0.003 \text{ kg/s}$).

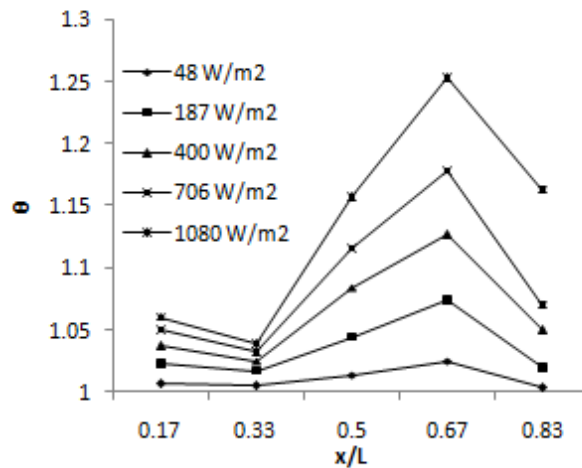


Figure (10) Effect of heat flux on the temp. ratio distribution along the enclosure at ($\dot{m} = 0.03$ kg/s).

Figures (11-15) illustrate the effect of changing mass flow rate at a specific heat flux on the local Nusselt number (Nu_x) along the enclosure. The density of the hot air is small so the hot air gets lighter and rises up. At ($\frac{x}{L} = 0.33$) - the coldest region- the highest heat convection is occurred and the highest Nu_x is observed because of the high temperature difference between the air and the surface. Where at ($\frac{x}{L} = 0.67$) - the hottest region- the heat convection is the smallest since the hot air convects less heat when the surface temperature is close to its temperature – low temperature difference between the air and the surface. Also from these figures it can be observed that when the water flow rate increases more heat is convected through the enclosure which means higher Nu_x .

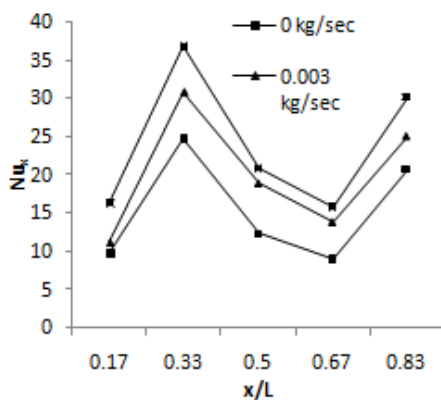


Figure (11) Effect of mass flow rate on local Nusselt distribution along the enclosure at ($Q_g = 48$ W/m²).

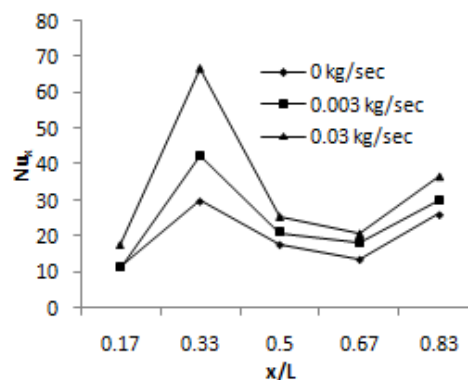


Figure (12) Effect of mass flow rate on local Nusselt distribution along the enclosure at ($Q_g = 187$ W/m²).

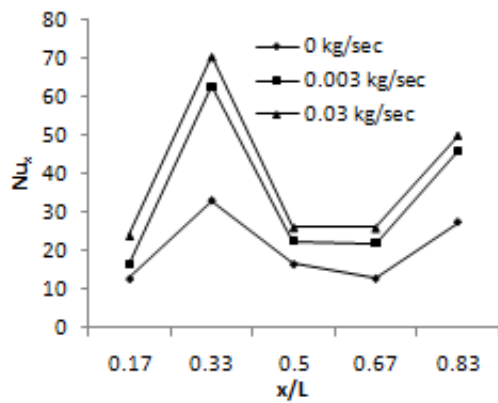


Figure (13) Effect of mass flow rate on local Nusselt distribution along the enclosure at ($Q_g=400 \text{ W/m}^2$).

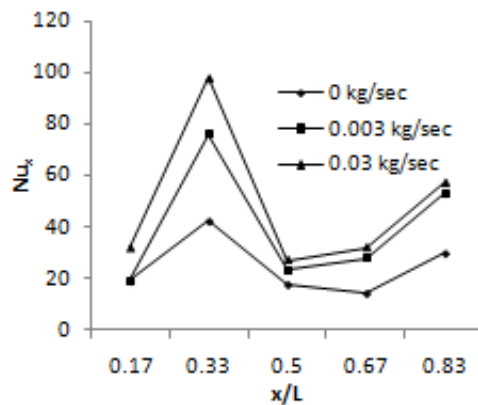


Figure (14) Effect of mass flow rate on local Nusselt distribution along the enclosure at ($Q_g=706 \text{ W/m}^2$).

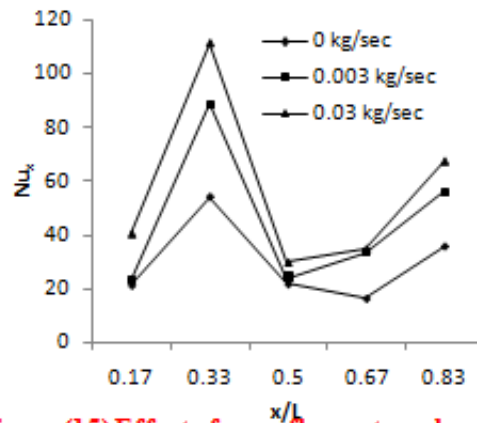


Figure (15) Effect of mass flow rate on local Nusselt distribution along the enclosure at ($Q_g=1080 \text{ W/m}^2$).

No different behavior is observed if the heat flux changed as shown in figures (16-18) – where the effect of changing the heat flux on the Nusselt number (Nu_x) along the enclosure is shown-. As was expected; more heat flux added to the enclosure means more heat convected through it.

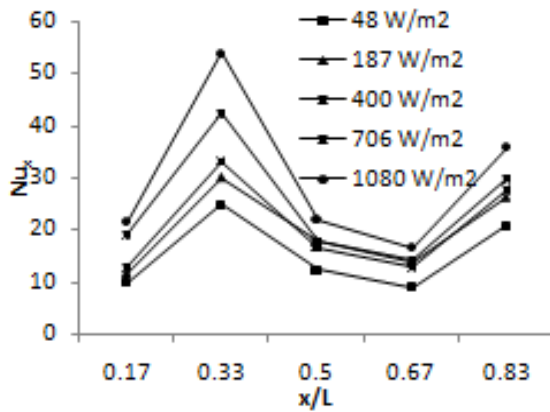


Figure (16) Effect of heat flux on local Nusselt distribution along the enclosure at ($\dot{m} = 0$ kg/s).

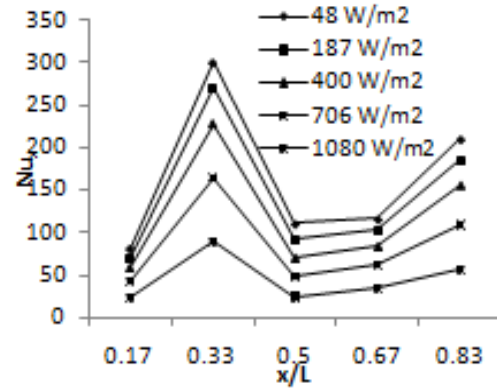


Figure (17) Effect of heat flux on local Nusselt distribution along the enclosure at ($\dot{m} = 0.003$ kg/s).

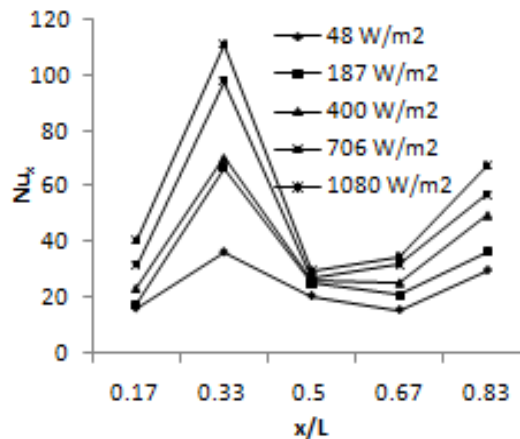


Figure (18) Effect of heat flux on local Nusselt distribution along the enclosure at ($\dot{m} = 0.03$ kg/s).

Figure (19) shows the relationship between the average Nusselt number and the average Rayleigh number for different values of water mass flow rates. It could be seen that the average value of Nusselt number is increasing with the increase of average Rayleigh number and this is for all different water mass flow rates, this causes increasing the heat transfer coefficient. When the mass flow rate is small the water gets hotter and the heat transfer reduced and Nu will be reduced subsequently.

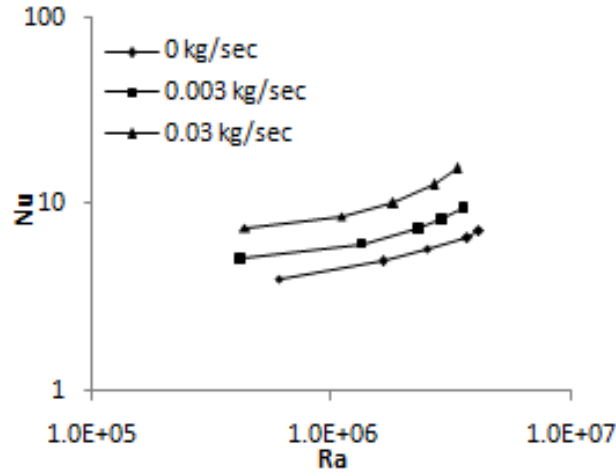


Figure (19) Average Nusselt number versus Raleigh numbers at different mass flow rates.

The following correlation is obtained for the present data:

$$Nu = 0.216 Ra^{1/4} \quad (11)$$

For $(4 \times 10^5 \leq Ra \leq 4 \times 10^6)$; with an error band of $(\pm 30\%)$.

Figure (20) compares the regression of the lines and experimental data; beside the comparison between the correlation obtained (eq.11) with (eq.10), it can be seen the error percentage doesn't exceed (21%), which can be accepted.

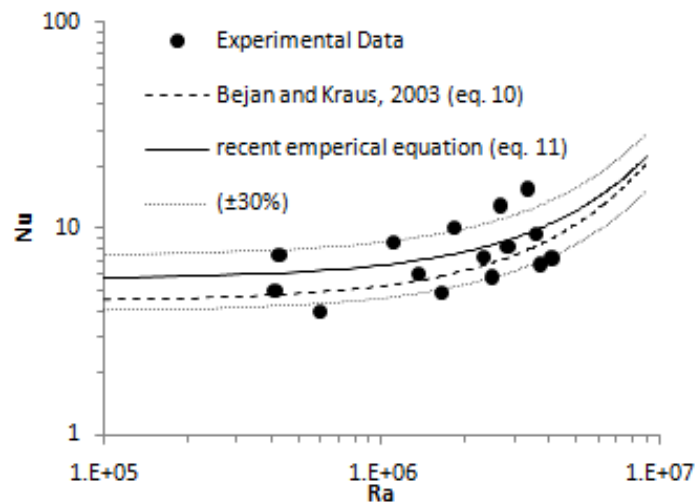


Figure (20) comparison between present experimental data with the correlation obtained (eq.11) and (eq.10).

Conclusions

Natural convection has been investigated experimentally in a vertical enclosure; one of its vertical surfaces is heated from its lower half while the upper was cooled, for Rayleigh number range ($4 \times 10^5 \leq Ra \leq 4 \times 10^6$). The following conclusions can be dictated:

- The highest Nu_x is found at ($\frac{x}{L} = 0.33$) where the coldest region is formed- high temperature difference between the air and the surface- , while the lowest Nu_x is found at ($\frac{x}{L} = 0.67$) where the hottest region is formed.
- Increasing the mass flow rate helped in absorbing more heat and subsequently increasing the heat transfer from the enclosure which means higher Nu.
- Increasing the heat flux increases the amount of heat provided to the enclosure which leads to increase Nu.

Nomenclature

A_s	Surface area of test section (m^2)
B	Enclosure width (m)
C_p	Specific heat ($J.kg^{-1}.K^{-1}$)
G	gravitational acceleration (ms^{-2})
h_x	Local Convection Heat transfer coefficient ($W.m^{-2}.^{\circ}C^{-1}$)
\bar{h}	Average Convection Heat transfer coefficient ($W.m^{-2}.^{\circ}C^{-1}$)
I	Electrical current (A)
K	Thermal conductivity ($W.m^{-1}.^{\circ}C^{-1}$)
L	Enclosure length (m)
\dot{m}_w	Mass flow rate of water ($kg.s^{-1}$)
Q_g	Heat generated ($W. m^{-2}$)
q_c	Convection heat flux ($W. m^{-2}$)
q_r	Radiation heat flux ($W. m^{-2}$)
Q_w	Cooling heat (Watt)
T	Temperature ($^{\circ}C$)
V	Heater voltage (V)
X	Axial distance (m)

Dimensionless Group

Nu Nusselt number

Ra Rayleigh number

Greek symbols

α Thermal diffusivity ($\text{m}^2 \text{s}^{-1}$)

β Volume expansion coefficient (K^{-1})

Δ Enclosure thickness (m)

E Emissivity

Θ temperature ratio between the surface temperature and the temperature of the air in the center of the enclosure

N Kinematic viscosity ($\text{m}^2 \cdot \text{s}^{-1}$)

Σ Stefan-Boltzmann constant = 5.67×10^{-8} ($\text{W m}^{-2} \text{K}^{-4}$)

Subscripts

C Cold surface

F Film

H Hot surface

i Inlet

O Outlet

W Water

References

1. M.Raos, (2001) Numerical investigation of laminar natural convection in inclined square enclosures, FACTA universitatis, series: physics, chemistry and technology, 2, 149-157.
2. G.Desrayaud, and A.Alberto Fichera (2002) Laminar natural convection in a vertical isothermal channel with symmetric surface-mounted rectangular ribs, International Journal of Heat and Fluid Flow, 23, 519–529.
3. da Silva, A. K., Lorenzini, G. and Bejan, A. (2005) Distribution of heat sources in vertical open channels with natural convection, International Journal of Heat and Mass Transfer, 48, 1462-1469.
4. G. Tanda, (2008) Natural convective heat transfer in vertical channels with low-thermal-conductivity ribs, International Journal of Heat and Fluid Flow, 29, 1319-1325.

5. A.BaIri, Garcia de Maria¹, J. M., Laraqi, N. and Alilat, N. (2008) Free convection generated in an enclosure by alternate heated bands. Experimental and numerical study adapted to electronics thermal control, International Journal of Heat and Fluid Flow, 29, 1337-1346.
6. M. P.Nimkar, and S. V.Prayagi, (2011) Heat transfer by natural convection in two vertical and one horizontal plate – an overview, International Journal of Engineering Science and Technology (IJEST), 3, 1008- 1013.
7. A.Bejan, and A. D. Kraus, (2003).Heat Transfer Handbook, John Wiley & Sons.
8. R.Siegel, and J. R. Howell, (1992) Thermal Radiation Heat Transfer, McGraw-Hill,New York, 3rd edition.
9. J. P. Holman, (1977) Experimental Method for Engineers, McGraw- Hill Book company, 5th Edition.
10. E. A. Mohamed (2007) Experimental study of steady state natural convection heat transfer from noncircular metallic ducts, King Saud university, college of engineering research center, No. 33/426.